

## Development of Lithium Bromide-Water Absorption Heat Pump System for Simultaneous Production of Heated-up Air and Steam From Waste Heat

Marumo K., Kobayashi N. and Itaya Y.\*

\*Author for correspondence

Department of Mechanical Engineering,  
 Gifu University,  
 Gifu 501-1193,  
 Japan,  
 E-mail: yitaya@gifu-u.ac.jp

### ABSTRACT

Absorption heat pumps (AHPs) operate by refrigeration techniques that use heat without requiring a compressor. In this study, an innovative AHP system is proposed that uses waste heat at 80 °C to produce hot air (at least 120 °C), which can be used for applications such as drying, and to simultaneously generate steam of 100–115 °C. Air is heated directly by heat exchange in the absorber working in the heating mode of a LiBr/H<sub>2</sub>O AHP system. Steam is then produced by heat exchange with the absorption solution, which is still at high temperature. The performance of a bench-scale AHP was evaluated by examination of running in a continuous mode. The tested AHP achieved a hot air temperature of more than 120 °C at the outlet of the absorber, and steam up to 115 °C was simultaneously generated by recovering heat from 80 °C hot water. The coefficient of performance, which is defined as the ratio of heat generated to the power consumed for pumping fluid, exceeded 20. The heat transfer rate in the absorber was dominated by an air stream through a bundle of tubes, but temperature in the evaporator was a significantly sensitive factor for the increasing temperature in this proposed AHP system.

### INTRODUCTION

The petrochemical and steel industries are the most energy-intensive manufacturing industries by a significant margin. Waste heat at a temperature level of 60–90 °C is generated by the industrial processes of these industries in large quantity. Research and development of the recovery of such waste energy is essential and important for effective utilization of energy. Absorption heat pumps (AHPs) operate by refrigeration techniques that use heat without requiring a compressor [1–4]. AHPs have been recently applied to steam generation and increasing heat levels of hot water by recovering waste heat [5–

9]. However, the need for steam with pressures as low as 0.2 MPa is not strong in industry.

### NOMENCLATURE

$A$	[m <sup>2</sup> ]	Heat transfer surface area
COP	[-]	Coefficient of performance
$C_p$	[J/(kg·K)]	Specific heat
$D_o$	[m]	Outside diameter of tube
$G_c$	[kg/s]	Mass flow rate of air
$H$	[J/kg]	Specific enthalpy
$\dot{M}$	[kg/s]	Mass flow rate
$\dot{m}$	[kg-H <sub>2</sub> O/(m <sup>2</sup> ·s)]	Rate of absorption or evaporation
$\dot{Q}$	[W]	Heat transfer rate
$Re_A$	[-]	Reynolds number
$T$	[K]	Temperature
$U_A$	[W/m <sup>2</sup> ·K]	Overall heat transfer coefficient
$w$	[W]	Input power for pumps
$\Delta T$	[K]	Temperature difference
$z$	[m]	Cartesian axis direction

### Special characters

$\rho$	[wt%]	Concentration of LiBr in solution
$\mu_A$	[Pa·s]	Viscosity of air

### Subscripts

1	Inlet of fluid
2	Outlet of fluid
$A$	Absorber or air
$C$	Condenser
$E$	Evaporator 1
$E2$	Evaporator 2
$G$	Generator

<i>g</i>	Gas phase (air or steam)
<i>h</i>	Input heat base
<i>i</i>	Inside of tube
<i>o</i>	Outside of tube
<i>p</i>	Input pump power base
<i>S</i>	Absorption solution
<i>W</i>	Water

A novel steam generation system has been proposed to recover waste hot water (80 °C) and to yield steam hotter than 150 °C by using a water-zeolite adsorption heat pump [10]. The performance of that system has been evaluated for a bench-scale system [11]. The system introduces direct contact of water to zeolite to yield high temperature compressed steam in the steam generation step as well as direct drying of zeolite by a hot air stream in the bed to reduce the desorption time by means of efficient heating in the regeneration step. This requires dry air hotter than 120 °C to sufficiently regenerate zeolite saturated with water. In recent years, CO<sub>2</sub> hot blast heat pump which generates 120°C air was developed. Compared with an oil-fired boiler, this new heat pump can reduce CO<sub>2</sub> emissions and running costs by about 41% each year.

In this study, an innovative LiBr/water AHP system is suggested for heating waste heat from 80 °C and simultaneously producing hot air at temperatures over 120 °C, which would then be available for the zeolite regeneration, and steam of 100–115 °C for preheating the bed of zeolite due to its adsorption prior to the steam generation step. Air is heated directly by heat exchange in the absorber working in the heating mode of an AHP. Steam is then generated by recovering heat in the absorption solution which is still at a high temperature. This system can be driven by thermal energy, consuming only a

little electricity for pumping fluid. However, heat transfer between air and a heating surface is generally much lower than heating or boiling water streaming on the surface. To address this, a LiBr/water solution is supplied so that it flows down and forms a film along the inside wall of spiral tubes set vertically while air flows among the bundle of tubes in the absorber. This structure can enlarge the heat transfer surface area and allows directly enhancing the heat transfer rate by increasing the number of tubes and introducing a turbulence promotion effect on the surface of the spiral tubes. The present work examines the performance of a bench-scale AHP system to determine the heat transfer parameters necessary to design a larger-scale system. In the case which generated only 120°C air by the innovative AHP system, compared with an oil-fired boiler, this new heat pump can reduce CO<sub>2</sub> emissions and running costs by about 98% each year.

## EXPERIMENT

Figure 1 shows a schematic diagram of flow in the experimental apparatus. The main structure of the present AHP system was composed of an evaporator (evaporator 1), an absorber, a regenerator, a condenser, an evaporator (evaporator 2), a solution heat exchanger, solution pumps, and water pumps. Tubes of the heat exchanger employed in the AHP system are of spiral and bare types (Figure 2); the specifications are listed in Table 1. The absorbent used in the AHP was an aqueous solution of lithium bromide (LiBr). All operational processes took place in a closed system under sealed evacuated atmosphere. The absorbent solution condensed in the regenerator was fed to the absorber by a pump through the

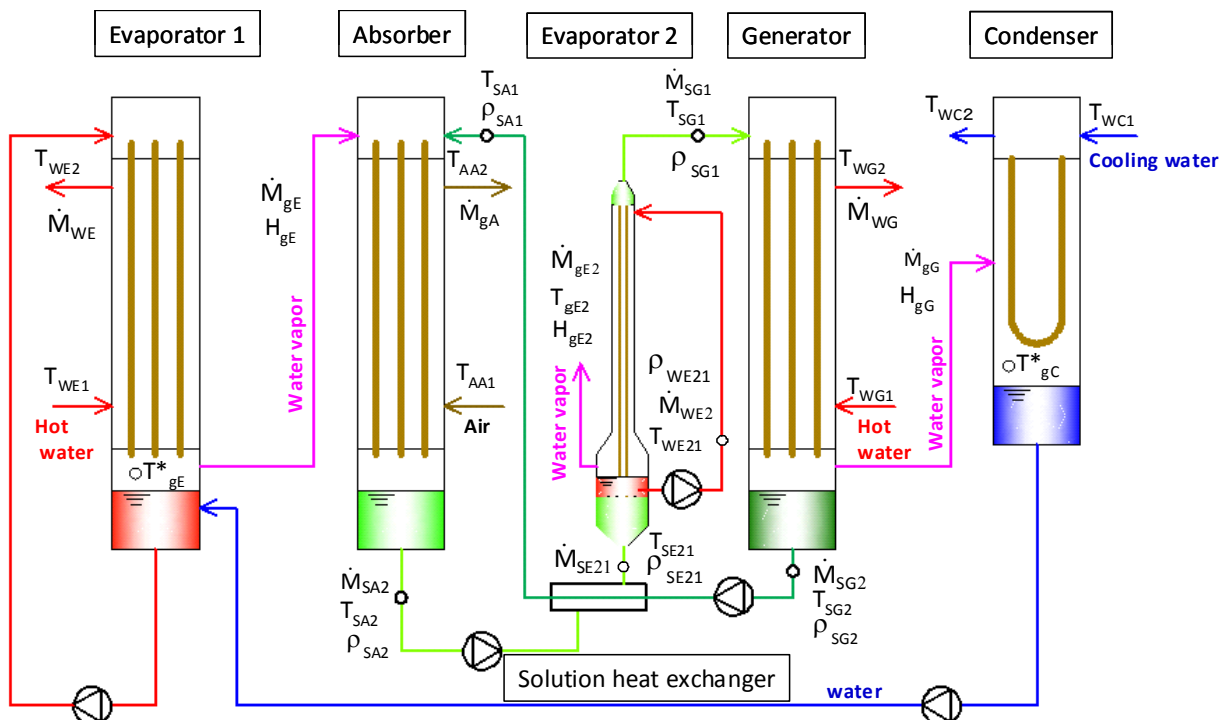
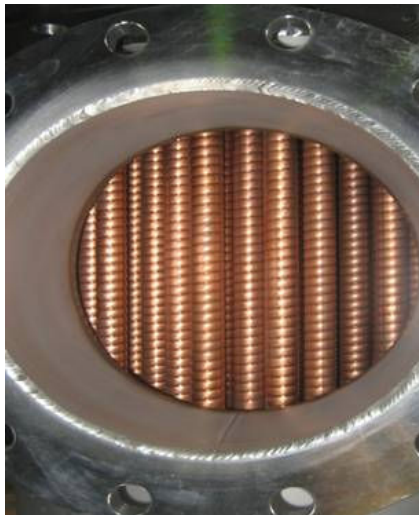


Figure 1 Schematic diagram of flow in experimental apparatus



(a) Spiral tubes



(b) Bare tubes

**Figure 2** Heat transfer tubes used in AHP system

**Table 1** Tubes of heat exchanger of AHP

Element	Evaporator 1	Absorber	Generator	Condenser	Evaporator 2
Material	Copper	Copper	Copper	Copper	Copper
Number of tubes	74	46	42	91	4
Length (mm)	4848	4940	4352	5500	3200
Inner diameter (mm)	23	23	23	16.6	16.6
Shape	Vertical spiral tubes	Vertical spiral tubes	Vertical spiral tubes	U-shaped bare tubes	Vertical bare tubes

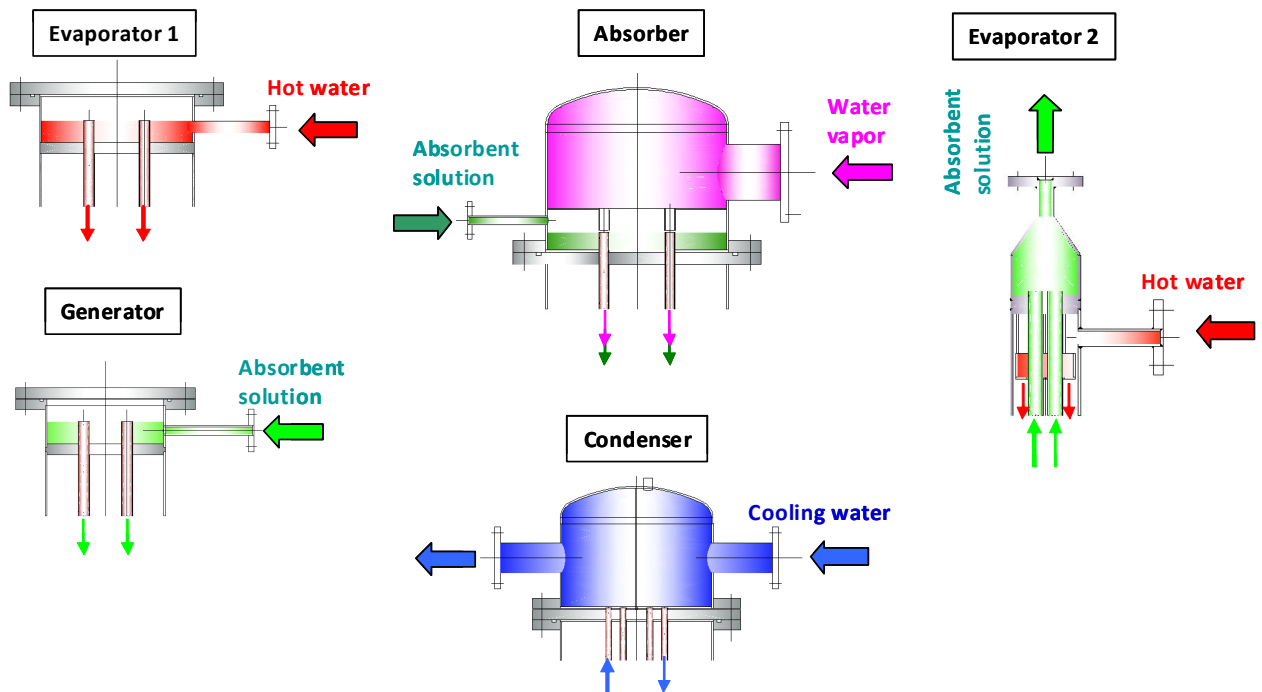


**Figure 3** Structures of the upper part of each apparatus

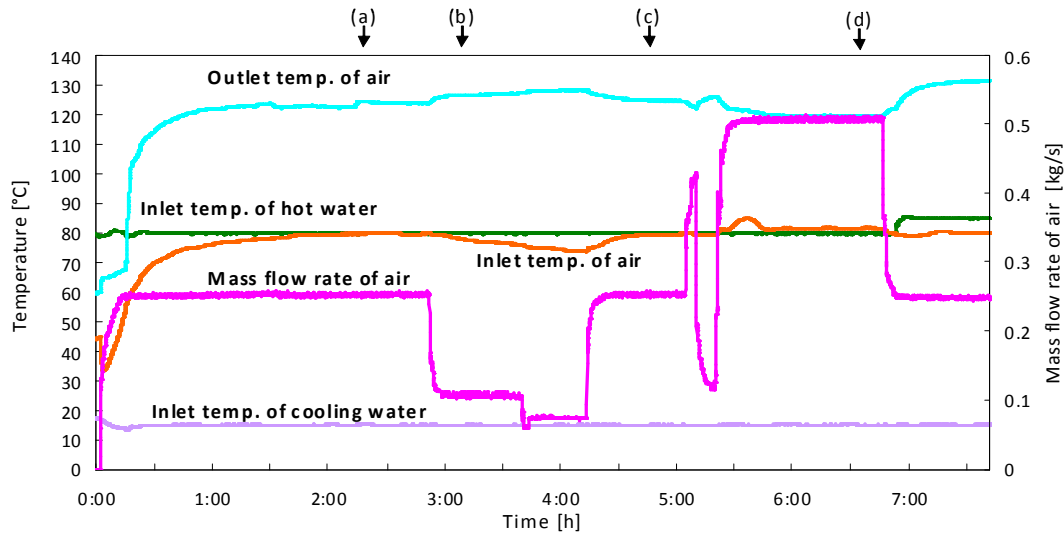


**Figure 4** Time variation of temperature in absorber of AHP

Hot water mass flow rate: 9.9 kg/s

Cooling water mass flow rate: 7.2 kg/s

solution heat exchanger. A film of the solution flowing down the inside wall of the vertical tubes was formed in the absorber to absorb water vapor from the evaporator. In the evaporator, vapor was evaporated on a pure water film flowing on the inside wall of the tubes heated by hot water at 80 °C, which flowed around the tubes. The detailed structures are shown in Figure 3. Then, the solution was heated during downward flow due to an increase of exothermic dilution heat in the solution and the latent heat by water vapor absorption. Air streamed in a counter flow around the tubes in the absorber, and heat exchange took place to heat the air through the tubes from the solution.

The absorbent solution diluted by absorbing water vapor was passing through the solution heat exchanger and an evaporator (evaporator 2) for heat recovery prior to returning into the generator. In evaporator 2, steam was then produced from a film of pure water flowing on the outside wall of the tubes heated by absorption liquid, which still had a high temperature. In the generator, the absorbent solution flowed down, forming a film on the inside wall of the tubes, and was heated by hot water (80 °C), which flowed around the tubes. The solution was condensed during downward flow by evaporation of water vapor. The evaporated water vapor transferred into the condenser, and was condensed on the surface of the tubes, which were cooled by water fed into the inside. The water in the condenser was returned to the evaporator. The performance of the AHP was monitored continuously during its operation. When it was confirmed that the operation achieved a sufficiently steady state, the temperatures of the fluids were measured at the inlet and outlet of each device. The absorbent solution was sampled at the inlet and outlet of the absorber to determine the concentration of LiBr by using an infrared moisture analyzer (Shimadzu MOC-120H).

## RESULTS AND DISCUSSION

### Heating Behavior of Hot Air in Absorber

Figure 4 shows the time behavior of the outlet temperature of hot air heated in the absorber of the AHP. The mass flow rates of hot water supplied to the evaporator and cooling water to the condenser were fixed at 9.9 kg/s and 7.2 kg/s, respectively. Inlet temperatures of the hot water and the cooling water are also marked in the figure. The outlet temperature of the air in the absorber was heated more than 120 °C without significantly influencing the mass flow rate of air, which was fed in the range of 0.08 to 0.5 kg/s. The air temperature was influenced, rather, by hot water temperature in the evaporator; the air temperature reached 130 °C when the hot water temperature had risen by only 5 °C.

The overall heat transfer coefficient  $U_A$  in the absorber was estimated from the experimental results by

$$U_A = \dot{Q}_A / (\Delta T_A A), \quad (1)$$

where the heat transfer rate  $\dot{Q}_A$  and mean temperature difference  $\Delta T_A$  are determined as shown in Table 2. Specific enthalpy of the solution can be found as a function of temperature and the concentration by consulting the references [2, 3].

Figure 5 shows the overall heat transfer coefficient in the absorber against the Reynolds number for the air stream flowing through the bundle of tubes, which is given by

$$Re_A = D_o G_c / \mu_A, \quad (2)$$

where  $D_o$  is the outside diameter of the tubes,  $G_c$  is the maximum mass flow rate of air through a bundle of tubes, and  $\mu_A$  is air viscosity.

The symbols (a), (b), (c), and (d) in Figure 5 correspond to the conditions labeled in Figure 4. The overall heat transfer coefficient rose with an increase in  $Re$  or the air flow rate. This

implies that the heat transfer between the LiBr aqueous solution and air may be dominated by convective heat transfer into air on the outside walls of the tubes in the absorber. The overall heat transfer coefficient was compared with heat transfer coefficients predicted for both sides of the tubes by previously reported empirical correlations to verify the heat transfer mechanism. Heat transfer in a liquid film flowing down a vertical tube wall occurs according to a formula of Wilke [12]. The convective heat transfer coefficient for air flowing through a bundle of tubes was predicted by Bell [13].

The predicted convective heat transfer coefficient between air and the outside walls of the tubes and the overall heat transfer coefficient, determined from conduction through tube walls and convection on both sides of the tubes, are also plotted in Figure 5. The overall heat transfer coefficient was almost the same as the convective heat transfer coefficient on the outside of the tubes. These results reveal that convective heat transfer between the air and the tubes dominates the overall heat transfer, as noted above. The dependency of the Reynolds number on the overall heat transfer coefficient obtained by examination was somewhat different than the predicted dependency because the heat transfer mechanism through spiral tubes in the absorber is more complicated than the analogous problem for bare tubes, which can ignore the exothermic reaction in the solution. However, the magnitudes became reasonably close at  $Re=4000$  with respect to the average temperature difference, defined by  $\Delta T_A$  in Table 2.

The coefficients of performance,  $COP_p$  and  $COP_h$ , of the AHP, which were calculated by the equation in Table 2, are plotted in Figure 6.  $COP_p$  based on the electric power used to pump fluid was enhanced by increasing  $Re$  and was greater than 20 when  $Re_A$  was greater than 3000.  $COP_h$  corresponds to thermal efficiency, and is based on the total input energy.  $COP_h$  reached as high as 30% for  $Re_A$  above 3000.

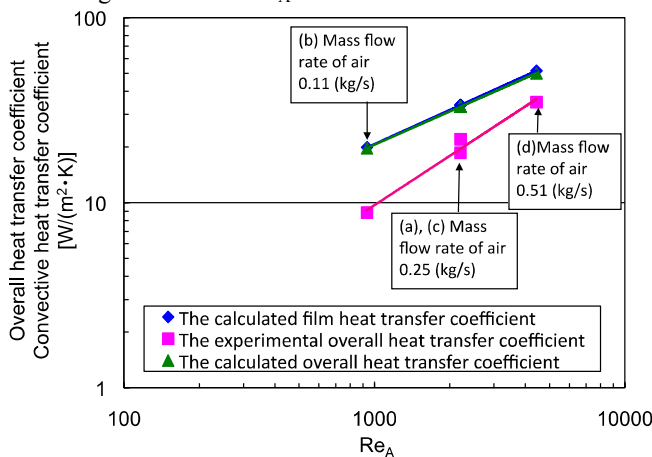


**Figure 5** Effect of the mass flow rate of air on heat transfer coefficient (for the case shown in Figure 4)

### Simultaneous Hot Air Heating and Steam Generation

The simultaneous heating of air and generation of steam was evaluated. Figure 7 shows the time behaviors of temperatures in the absorber and evaporator 2 of the AHP. Hot air (80 °C inlet) was heated to 125 °C in the absorber and saturated steam

at 100 °C was simultaneously generated at a rate of 0.0047 kg/s under atmospheric pressure in evaporator 1. When steam generation is regulated to 0.0025 kg/s, the steam temperature reached 115 °C and the hot air temperature remained at 125 °C.

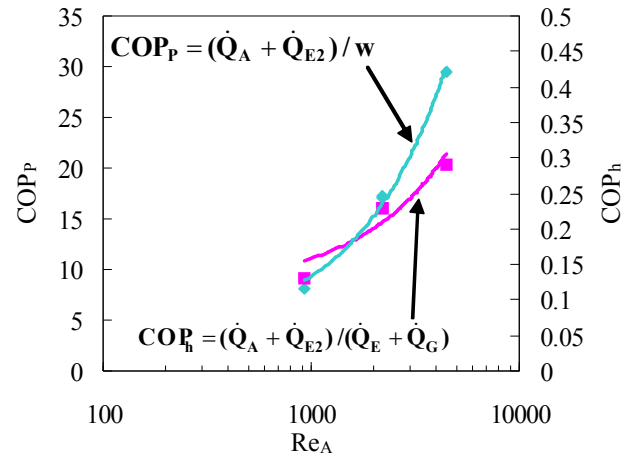


**Figure 6** Effect of the mass flow rate of air on COP

Figure 8 shows the influence of steam generation temperature on the total COP.  $COP_p$  for only hot air obtained without steam generation was 17; under the same operating conditions in combination with steam generation, this improved  $COP_p$  to over 20 although, the magnitude was reduced at increasing steam temperatures.

## CONCLUSION

An innovative LiBr/water AHP system was developed to use waste heat at 80 °C to simultaneously produce air hotter than 120 °C and steam. The results obtained by examination of a bench-scale system and the numerical analysis can be summarized as by the following points:

1. Air was successfully heated to over 120 °C by direct heat exchange in the absorber. The hot air temperature was significantly influenced by temperature in the evaporator, rather than by the mass flow rate of air.
2. The coefficient of performance, defined as the ratio of hot air energy to power consumed for pumping fluid, improved with an increase in air flow rate or Reynolds number and exceeded 15 for  $Re$  more than 10000.
3. Simultaneous hot air over 120 °C and steam up to 115 °C were obtained, as desired, and the coefficient of performance was greater than 20. Higher steam temperatures reduced the performance.

## ACKNOWLEDGMENT

The authors acknowledge financial support by the Research and Development Program for Innovative Energy Efficiency Technology under the New Energy and Industrial Technology Development Organization (NEDO) project based on a grant from the Japanese Ministry of Economy, Trade and Industry.

**Table 2**List of equations for AHP

Enthalpy change	
Evaporator 1	$\dot{Q}_E = C_{Pw}\dot{M}_{WE}(T_{WE1} - T_{WE2})$ $\dot{Q}_E = \dot{M}_{gE}(H_{gE} - H_{gC})$
Absorber	$\dot{Q}_A = C_{PA}\dot{M}_{AA}(T_{AA2} - T_{AA1})$ $\dot{Q}_A = \dot{M}_{gE}(H_{gE} - H_{SA2}) - \dot{M}_{SA1}(H_{SA1} - H_{SA2})$
Generator	$\dot{Q}_G = C_{Pw}\dot{M}_{WG}(T_{WG1} - T_{WG2})$ $\dot{Q}_G = \dot{M}_{gG}(H_{gG} - H_{SG1}) + \dot{M}_{SG2}(H_{SG2} - H_{SG1})$
Condenser	$\dot{Q}_C = C_{Pw}\dot{M}_{WC}(T_{WC2} - T_{WC1})$ $\dot{Q}_C = \dot{M}_{gG}(H_{gG} - H_{gC})$
Evaporator 2	$\dot{Q}_{E2} = \dot{M}_{gE2}(H_{gE2} - H_{WE2})$ $\dot{Q}_{E2} = \dot{M}_{SE21}H_{SE21} - \dot{M}_{SG1}H_{SG1}$
Heat pump	$COP_h = (\dot{Q}_A + \dot{Q}_{E2}) / (\dot{Q}_E + \dot{Q}_G)$
	$COP_p = (\dot{Q}_A + \dot{Q}_{E2}) / w$ w: Input power for pump
Mass balance	
Flow rate	$\dot{M}_{gE} = \dot{M}_{SA2} - \dot{M}_{SA1}$ $\dot{M}_{gG} = \dot{M}_{gE}$ $\dot{M}_{SG1} = \dot{M}_{SA2}$ $\dot{M}_{SG2} = \dot{M}_{SA2} = \dot{M}_{SE21}$
Concentration	$\rho_{SA2} = \rho_{SG1} = \rho_{SE21}$ $\rho_{SA1} = \rho_{SG2}$ $\dot{M}_{SG2} \cdot \rho_{SG2} = \dot{M}_{SG1} \cdot \rho_{SG1}$
Heat driving force	
Evaporator 1	$\Delta T_E = (T_{WE1} - T_{WE2}) / \text{Ln}\{(T_{WE1} - T_{gE}^*) / (T_{WE2} - T_{gE}^*)\}$
Absorber	$\Delta T_A = \{(T_{SAk} - T_{AA2}) - (T_{SA2} - T_{AA1})\} / \text{Ln}\{(T_{SAk} - T_{AA2}) / (T_{SA2} - T_{AA1})\}$
Generator	$\Delta T_G = \{(T_{WG1} - T_{SG2}) - (T_{WG2} - T_{SGk})\} / \text{Ln}\{(T_{WG1} - T_{SG2}) / (T_{WG2} - T_{SGk})\}$
Condenser	$\Delta T_C = (T_{WC2} - T_{WC1}) / \text{Ln}\{(T_{gC}^* - T_{WC1}) / (T_{gC}^* - T_{WC2})\}$
Evaporator 2	$\Delta T_{E2} = (T_{SE21} - T_{SG1}) / \text{Ln}\{(T_{SE21} - T_{gE2}) / (T_{SG1} - T_{gE2})\}$

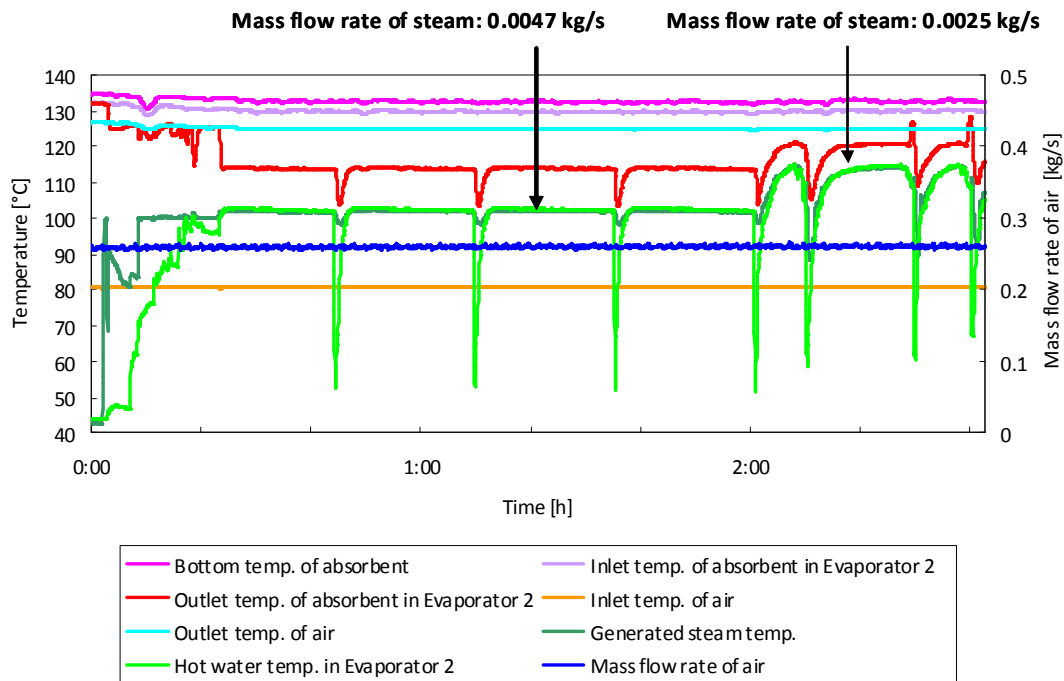


**Figure 7**Time behaviors of temperature in absorber and evaporator 2 of AHP.  
 Inlet hot water temp.: 80 °C    Hot water mass flow rate: 9.9 kg/s  
 Inlet cooling water temp.: 15 °C    Cooling water mass flow rate: 7.2 kg/s



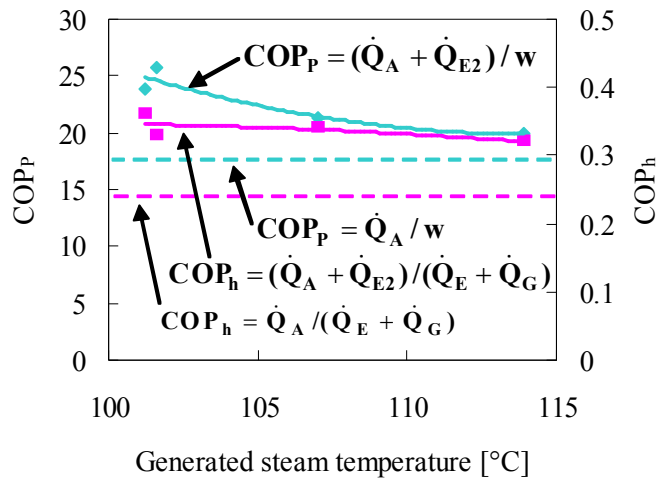


**Figure 8** Effect of the generated steam temperature on COP (air flow rate: 0.25 kg/s)

## REFERENCES

- [1] Florides G. A., Kalogirou S. A., Tassou S. A. and Wrobel L. C., Design and construction of a LiBr-water absorption machine, *Energy Convers. Manag.*, Vol. 44, 2003, pp. 2483-2508
- [2] Sun D. W., Thermodynamic design data and optimum design maps for absorption refrigeration system, *Appl. Therm. Eng.*, Vol. 17, 1997, pp. 211-221
- [3] Herold K. E., Radermacher R. and Klein S. A.; Adsorption chillers and heat pumps, CRC Press, 1996
- [4] Sencan A., Yakut K. A. and Kalogirou S. A., Exergy analysis of lithium bromide/water absorption systems, *Renewable Energy*, Vol. 30, 2000, pp. 645-657
- [5] Grossman G. and Childs K. W., Computer simulation of a lithium bromide-water absorption heat pump for temperature boosting, *ASHRAE Transactions*, Vol. 89-1, 1983, pp. 240-248
- [6] Fujii T., Development activities of low temperature waste heat recovery appliances using absorption heat pumps, 2010 International Symposium on Next-generation Air Conditioning and Refrigeration Technology, 17-19 February, 2010, Tokyo, Japan
- [7] Dong, T., Qian, B., Weng, J., Yu, X., Lithium Bromide-Water Absorption Heat Transformer Using 78 °C Waste Heat, *Proceedings of Absorption Heat Pump Conference*, 30 September-2 October, 1991, Tokyo, Japan, pp. 357-362
- [8] Ahachad, M., Charia, M., Absorption Heat Transformer Application Refrigerating Machine, *Proceedings of the International Absorption Heat Pump Conference*, 19-21 January, ASME AES-Vol.31, 1994, New Orleans, USA, pp. 101-108
- [9] Bisio, G., Pisoni, C., Thermodynamic Analysis of Heat Transformers, *Proceedings of Absorption Heat Pump Conference*, 30 September-2 October, 1991, Tokyo, Japan, pp. 315-320
- [10] Kawakami Y., Abe Y., Ito K., Marumo K., Aoyama T., Tanino M., Nakaso K., Nakagawa T., Itaya Y. and Fukai J., Development of Bench-Scaled Adsorption Type Steam Recovery System for Generating High Temperature Steam From Hot Waste Water, *Proceedings of the 2013 AIChE Annual Meeting*, San Francisco, CA, USA, November 3-8, 2013
- [11] Nakaso K., Nakashima K., Tanaka Y., Iwama Y. and Fukai J., Study On Performance of the Novel Steam Generation System Using Water-Zeolite Pair, *Proceedings of 2013 AIChE Annual Meeting*, San Francisco, CA, USA, November 3-8, 2013
- [12] Obana, H., Handbook for design of heat exchanger, Kogaku Tosho, 2000, pp. 688-691
- [13] Bell K. J., Exchanger design: Based on the Delaware research report, *Petro / Chem.*, Vol. 32, 1960, C26